Nanostructures

Deutsche Ausgabe: DOI: 10.1002/ange.201901913
Internationale Ausgabe: DOI: 10.1002/anie.201901913

Controlled Assembly of Block Copolymer Coated Nanoparticles in 2D Arrays

*Vanessa B. Leffler[+], Lina Mayr[+], Paul Paciok, Hongchu Du, Rafal E. Dunin-Borkowski, Martin Dulle, and Stephan Förster**

Abstract: *The defined assembly of nanoparticles (NPs) in polymer matrices is an important prerequisite for next-generation functional materials. A promising approach to control NP positions in polymer matrices at the nanometer scale is the use of block copolymers. It allows the selective deposition of NPs in nanodomains, but the final defined and ordered positioning of the NPs within the domains has not been possible. This can now be achieved by coating NPs with block copolymers. The self-assembly of block copolymer-coated NPs directly leads to ordered microdomains containing ordered NP arrays with exactly one NP per unit cell. By variation of the grafting density, the inter-nanoparticle distance can be controlled from direct NP surface contact to surface separations of several nanometers, determined by the thickness of the polymer shell. The method can be applied to a wide variety of block copolymers and NPs and is thus suitable for a broad range of applications.*

The defined assembly of functional nanoparticles in polymer matrices is highly desirable for the development of next-generation electrical, optical, memory, and energy conversion devices.[1] Currently, the lack of a precise control of nanoparticle positions, distances, and ordering in polymeric matrices is a severe barrier for many nanotechnology applications as these parameters sensibly determine mechanical, dielectric, magnetic, and plasmonic coupling as well as energy transfer in the active polymer matrices of the corresponding devices.

A versatile method to control nanoparticle locations and arrangements at the nanometer scale is the use of block copolymers.[2] For AB diblock copolymers, nanoparticles can be selectively integrated into the A or B domains, or into the A/B interface.[3] Early studies aiming at a domain selective integration involved either the synthesis of nanoparticles from precursors solubilized in the respective block copolymer domains, or used pre-synthesized nanoparticles.[4] Later improved methods employed nanoparticles which were surface compatibilized with the targeted polymer domain.

However, the controlled and stable incorporation of inorganic nanoparticles into polymer matrices remains difficult, because nanoparticles are thermodynamically immiscible with polymers. This is due to 1) unfavorable nanoparticle/polymer enthalpic interactions, and 2) a considerable loss of conformational entropy when polymer chains are located close to the nanoparticle surface.[5] The enthalpic interactions can be minimized by nanoparticle surface compatibilization with either polymer-compatible small molecules[6] or with polymers of the same type as the targeted block copolymer domain. As the conformational entropy of block copolymer chains is already reduced owing to their confinement at the domain interface, additional entropy losses owing to nanodomain incorporation immediately lead to problems of macrophase separation already at small volume fractions of nanoparticles.[7]

By using small molecules with attractive interactions such as hydrogen bonding[8] and ionic interactions,[9] which partially compensate entropy losses by negative enthalpic contributions, nanoparticle loadings of up to 40 wt % could be achieved. Coating the nanoparticles with a layer of the corresponding matrix polymer not only minimizes enthalpic interactions, but also significantly reduces the loss of conformational entropy of the polymer chains. With this method, even full thermodynamic miscibility of nanoparticles and polymers can be realized, such that highest loadings with the formation of ordered nanoparticle arrays can be achieved.[10]

The best method to localize nanoparticles in block copolymer domains would thus be the direct coating of the nanoparticles with the respective block copolymers. The attachment of block copolymers to nanoparticles has already been used for the fabrication of nanoparticles for biomedical applications.[11] However, the self-assembly of block copolymer coated nanoparticles into ordered arrays has, to the best of our knowledge, not yet been attempted or investigated.

Herein we show that the direct self-assembly of block copolymer coated nanoparticles, as opposed to homopolymer

[*] V. B. Leffler,[+] Dr. M. Dulle, Prof. Dr. S. Förster
JCNS-1/ ICS-1, Forschungszentrum Jülich GmbH
52425 Jülich (Germany)
E-mail: s.foerster@fz-juelich.de
V. B. Leffler,[+] Prof. Dr. S. Förster
Institute of Physical Chemistry, RWTH Aachen University
52074 Aachen (Germany)
L. Mayr[+]
Physikalische Chemie I, Universität Bayreuth
Universitätsstr. 30, 95440 Bayreuth (Germany)
Dr. P. Paciok, Prof. Dr. R. E. Dunin-Borkowski
ER-C-1/ PGI-5, Forschungszentrum Jülich GmbH
52425 Jülich (Germany)
Dr. H. Du
ER-C-2, Forschungszentrum Jülich GmbH
52425 Jülich (Germany)
and
GFE, RWTH Aachen University
52074 Aachen (Germany)
[+] These authors contributed equally to this work.
Supporting information and the ORCID identification number(s) for the author(s) of this article can be found under: https://doi.org/10.1002/anie.201901913.

 © 2019 Wiley-VCH Verlag GmbH & Co. KGaA, Weinheim

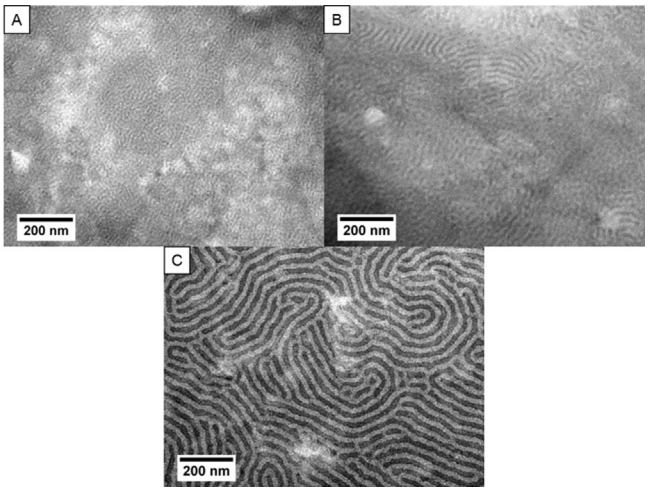

Figure 1. TEM images of the block copolymers dried from solution and stained with OsO_4; A) PI_{117}-PS_{80} (16 300 g mol^{-1}), B) PI_{226}-PS_{126} (28 500 g mol^{-1}), C) PI_{368}-PS_{225} (48 500 g mol^{-1}). All block copolymers show stripe-like morphologies.

coated ones, leads to thermodynamically stable, highly loaded 2D nanocomposites. It leads to the incorporation of exactly one nanoparticle per unit domain, and allows precise control of the inter-particle distance, which is of interest for sensing, electronic, catalytic, and lithographic applications.[12,13] Furthermore, the direct coupling of nanoparticle and block copolymer self-assembly leads to new morphologies that have not been reported and are otherwise difficult to access.

For a systematic study we investigated the self-assembly of block copolymer coated nanoparticles prepared from a series of three diblock copolymers that form lamellar phases in their neat state (Figure 1). From this we expected to obtain insights into the interplay of nanoparticle surface curvature and block copolymer interfacial curvature on the self-assembled morphology. We chose poly(styrene-*b*-isoprene) (PS-PI) block copolymers because their phase behavior has been well-established.[14] The block copolymers were synthesized by sequential living anionic polymerization to achieve a narrow molecular weight distribution and to functionalize the chain ends of the polystyrene blocks with coordinating end groups for stable attachment to the nanoparticle surfaces. For this, the living polystyrene chain ends were reacted with ethylene oxide to obtain PI-PS-OH block copolymers containing terminal OH groups. These were subsequently activated with carbonyl diimidazole and reacted with an excess of pentaethylene hexamine (PEHA), which acts as a multidendate ligand for a variety of chemically different nanoparticles. PEHA shows strong coordinative binding, but still possesses sufficient surface mobility to reach high grafting densities.[15] Monodisperse lead(II)sulfide (PbS),[16] zinc oxide (ZnO),[17] and iron oxide (Fe_2O_3)[18] nanoparticles were synthesized from their respective metal oleates. For the synthesis of the monodisperse Cu_2ZnSnS_4 (CZTS) nanoparticles we used a heat-up method.[19] The block copolymer molecular weights, compositions as well as the diameters of the nanoparticles are given in Table 1. For the synthesis of the block copolymer coated nanoparticles we used a recently developed ligand exchange method that allows the block copolymer grafting density to be controlled over a wide range via the concentration of polymeric ligand during ligand exchange.[15] The grafting density was determined by thermogravimetric analysis and is given in Table 1. Details of the synthesis and characterization of the nanoparticles and block copolymers are given in the Supporting Information.

For the present study we focused on two-dimensional assembly to obtain first insights into the coupled nanoparticle block copolymer self-assembly behavior. We used evaporation-induced self-assembly (EISA) to prepare monolayers in a reproducible and controlled way. To avoid any influence of solvent selectivity we chose cyclohexane and toluene as neutral solvents, where the block copolymer coated nanoparticle were dissolved at a concentration of 0.6 mg mL^{-1} prior to assembly on carbon-coated copper grids. Figure 1 shows that the neat block copolymers assemble into stripe domains as expected from the block length ratio and the published phase behavior.[14] The PI and PS domain sizes are in a range of 10 to 20 nm, which is comparable to the size range of the investigated nanoparticles.

As a first example we investigated the self-assembly of block copolymer coated 7 nm PbS-nanoparticles as a function of the molecular weight of the block copolymer. The observed nanocomposite morphologies are shown in Figure 2. We observe that the incorporation of nanoparticles significantly increases the degree of order of the block copolymer nanocomposites compared to the neat block copolymers (see Figure 1). As shown in Figure 2 A, for the smallest block copolymers the nanoparticles are arranged on a hexagonal lattice. The PS domains form a spherical shell around the nanoparticles and are fully separated from adjacent PS-domains by the PI matrix. This single nanoparticle per block copolymer domain structure has so far been very difficult to achieve otherwise[13] and shows the unique control of this method.

Table 1: List of block copolymer coated nanoparticles investigated herein.[a]

Label	Nanoparticle diameter [nm]	MW of block copolymer [g mol^{-1}]	Grafting density (TGA) [nm^{-2}]
$PbS_{7.2}$@PEHA-PS_{80}-PI_{117}_0.85	7.2 ± 0.9	16 300	0.85
$Fe_2O_{3;5.5}$@PEHA-PS_{126}-PI_{184}_0.16	5.5 ± 0.5	25 750	0.16
$Fe_2O_{3;5.5}$@PEHA-PS_{126}-PI_{184}_0.7	5.5 ± 0.5	25 750	0.7
$ZnO_{3.9}$@PEHA-PS_{126}-PI_{184}_0.79	3.9 ± 0.7	25 750	0.79
$CZTS_{13.7}$@PEHA-PS_{126}-PI_{226}_1.2_{theo}	13.7 ± 2.5	28 500	not determined
$Fe_2O_{3;6.7}$@PEHA-PS_{126}-PI_{226}_0.77	6.7 ± 0.5	28 500	0.77
$PbS_{4.9}$@PEHA-PS_{126}-PI_{226}_0.54	4.9 ± 0.7	28 500	0.54
$PbS_{7.2}$@PEHA-PS_{126}-PI_{226}_1.14	7.2 ± 0.9	28 500	1.14
$PbS_{7.5}$@PEHA-PS_{225}-PI_{368}_0.25	7.5 ± 1.1	48 500	0.25

[a] The lower index on the type of nanoparticles indicates the nanoparticle diameter in nanometers, the lower indices at the polymer block symbols denote the degrees of polymerization, and the last index denotes the grafting density in nm^{-2}.

 © 2019 Wiley-VCH Verlag GmbH & Co. KGaA, Weinheim

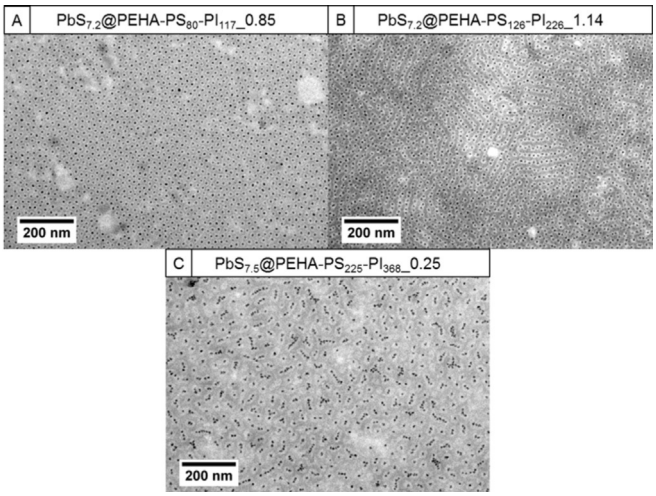

Figure 2. TEM images of PbS nanoparticles with a diameter of about 7 nm coated with PI-PS-PEHA block copolymer of different molecular weights. With increasing block copolymer molecular weight we observe a transition from single nanoparticles within spherical domains over single nanoparticles in strip-like domains to linear nanoparticle arrays in stripe-like domains.

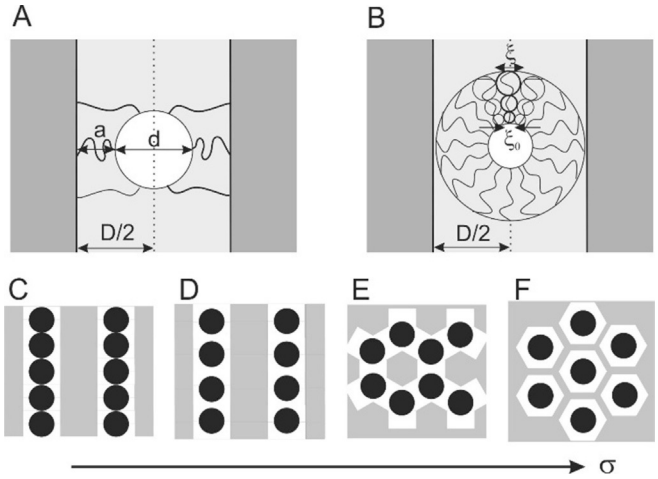

Figure 3. The localization of a nanoparticle in a stripe-like block copolymer domain to estimate the geometrical (A) and grafting density effects (B) on the degree of chain extension. The lower panel illustrates the sequence from surface-contact nanoparticle stripe domains (C) via polymer-separated nanoparticle stripe domains (D), Y-branched nanoparticle arrays with locally three-fold rotational symmetry (E) to hexagonally packed nanoparticle arrays (F) upon increasing grafting density σ.

Figure 2 B shows that for larger block copolymers the 2D lamellar morphology is retained. We observe ordered stripe domains where the nanoparticles arrange into linear arrays with regular periodic arrangement and well-defined inter-nanoparticle distance. So far, to our knowledge, this is the first report of this kind of nanostructure. It offers the unique possibility to precisely control distance-dependent inter-particle interactions in well-defined, ordered linear arrays.

Figure 2 C shows the possibility to also realize direct surface contact of adjacent nanoparticle in linear arrays when the block copolymer grafting density is sufficiently low. Direct contact of nanoparticles requires sufficient surface mobility of the ligands to decrease the ligand density at the contact area and to increase the ligand density outside, which stabilizes linear nanoparticle arrays.[20] This shows the potential of the method to also realize direct nanoparticle contact enabling direct directed charge, heat or energy transfer.

The formation of stripe and spherical domains can by rationalized by considering the loss of conformational entropy caused by the domain confinement of the polymer-coated nanoparticles. First, to homogeneously fill the volume of a stripe domain, the polymer blocks attached to the nanoparticle surface in the center of the domain need to extend over an end-to-end distance $D/2$ to connect to the interface, where D is the thickness of the domain (see Figure 3 A). In relation to the shortest distance a between nanoparticle surface and stripe interface, the polymer chains are extended by a factor $\alpha = D/(2a) = 1/(1-d/D)$, which is proportional to the deformation energy of the polymer chain.

Therefore, for larger block copolymers forming larger domains ($d \ll D$) there is negligible chain extension, whereas for smaller block copolymers with smaller domains the extension is considerable, leading to destabilization of stripe domains and the formation of spherical domains as observed in Figure 2.

Second, we observe a profound influence of the grafting density. Using a blob model as developed for star polymers,[21] we can estimate the size of the outer blob ξ, which needs to be of the order of $D/2$ for a chain to connect to the polymer interface. The ratio $\beta = D/(2\xi)$ is then proportional to the corresponding chain extension. Since $\xi = D\xi_0/d$ and because the inner blob size ξ_0 is related to the grafting density σ as $\xi_0{}^2 = 1/\sigma$, the factor β is given by $\beta = \sigma^{1/2}d/2$. Therefore for higher grafting densities and larger nanoparticles there is a preference for the formation of spherical domains, which is in good agreement with the observations in Figure 2 and 4. Stripe domains with periodic linear nanoparticle arrays are favored for smaller nanoparticles with intermediate grafting densities, whereas for larger nanoparticles and higher grafting densities transitions to more spherically symmetric nanoparticle arrangements are expected as shown in Figure 3 C–F.

As we observed a profound influence of the block copolymer grafting density on the self-assembled morphology in the first experiments, we investigated its effects over a wider range of grafting densities. Figure 4 A shows that for low grafting densities nanoparticles are in direct contact, forming chains and branched chain networks within the block copolymer domains. An increased grafting density leads to non-branched linear chains of surface contacted nanoparticles, with some regions where nanoparticles are already slightly separated (Figure 4 B). Further increasing the grafting density leads to the previously observed linear arrays of regularly separated nanoparticle as shown in Figure 4 C. Still higher grafting densities considerably increase the nanoparticle separation with a transition from linear to Y-branched PS domains such that locally nanoparticles start to arrange in five- or six-membered rings, which is a morphology that has also never been reported before.

 © 2019 Wiley-VCH Verlag GmbH & Co. KGaA, Weinheim

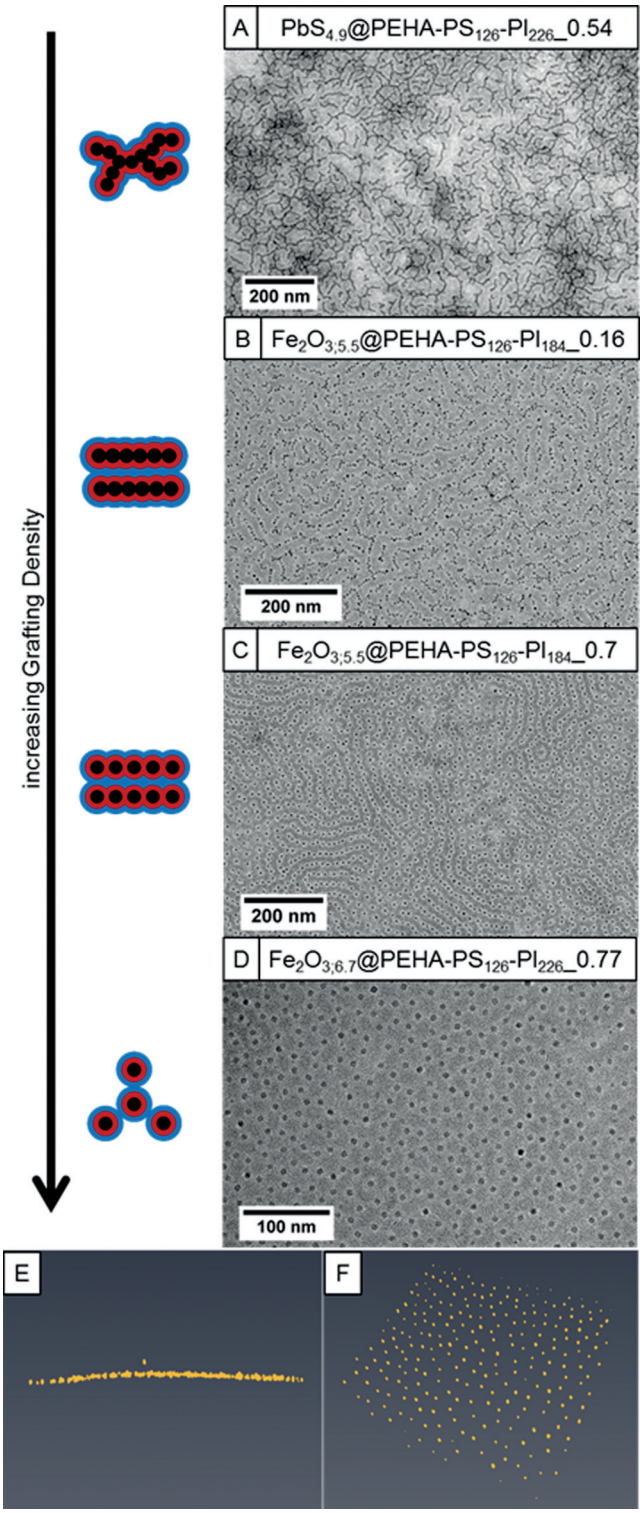

Figure 4. A)–D) TEM images of a series of different types of nanoparticle arrays that can be realized by variation of grafting density and nanoparticle/polymer size ratio. The arrays in (C) and (D) have been realized for the first time and represent the ideal case of exactly one nanoparticle per unit cell. E),F) 3D reconstruction of (D) by means of tomography. E) shows a side view and F) a slightly tilted top view to prove a two-dimensional arrangement.

This transition is related to a tendency to form more spherically symmetric arrangements around nanoparticles with increasing grafting density. Linear chain nanoparticle arrangements have a locally 2-fold rotational symmetry, which increases to a 3-fold rotational symmetry in case of the Y-branched arrangements as observed in Figure 4D. This is supported from a detailed analysis of the bond-orientational order as outlined in the Supporting Information. The bond orientational order for the linear array has a clear maximum at a value of 2 (Supporting Information, Figure S2), whereas for the Y-branched arrangement the maximum is clearly at a value of 3 (Supporting Information, Figure S1). We have performed STEM tomography (Figure 4E,F) to confirm that the arrangement shown in Figure 4D is two-dimensional. The corresponding perfect lattice would be a honeycomb lattice. With further increasing grafting density we would expect the formation of a 6-fold symmetric arrangement as in Figure 2A. With increasing rotational symmetry the PS-blocks become more localized around the nanoparticles which reduces the connectivity to adjacent nanoparticle domains. Thus, for the 3-fold rotational symmetry there are still connections to adjacent nanoparticles, whereas for the 6-fold rotational symmetry the PS-domains are completely separated and singly dispersed in a PI-matrix. The transition from locally 2-fold by 3-fold to 6-fold rotational symmetry in 2D is topologically similar to the transition from lamellar via gyroid to a hexagonal cylindrical arrangement in 3D bulk block copolymers.

To demonstrate the broad applicability of our approach, we not only showed the self-assembly into ordered nanoparticle block copolymer arrays for semiconducting PbS-nanoparticles (Figures 2, 4) and magnetic Fe_2O_3-nanoparticles (Figure 4), but also for semiconducting ZnO- and Cu_2ZnSnS_4-nanoparticles for a range of sizes, shapes, and polydispersities, which is shown in the Supporting Information.

We could demonstrate that the coating of nanoparticles with block copolymers is a general and versatile method to prepare well-defined 2D nanoparticle assemblies. The experiments together with a geometrical model show that the nanoparticle/domain size ratio and the grafting density are the two most important factors that control the type of block copolymer domain structure and the inter-particle distance. Linear nanoparticle arrays and superlattices with 2-fold, a newly discovered 3-fold, and 6-fold rotational symmetry can be formed for a variety of semi-conducting (PbS, ZnO, Cu_2ZnSnS_4) and magnetic (Fe_2O_3) nanoparticles. The method opens the way to the controlled preparation of well-defined complex nanoparticle arrays in polymer matrices with precisely one nanoparticle per unit domain, and a domain-selective localization such that ordered binary or ternary nanoparticle arrays can be achieved as would be necessary for example, for scintillation materials.

Experimental Section

All TEM samples for the assembly were prepared from a toluene (or cyclohexane) solution. The TEM grid was immersed in 8 µL of solution and after drying stained with OsO_4.

The nanoparticle and the polymer syntheses are depicted in the Supporting Information.

 © 2019 Wiley-VCH Verlag GmbH & Co. KGaA, Weinheim

Acknowledgements

Financial support of the SFB 840 is gratefully acknowledged. The authors thank the ER-C for providing access to the electron microscope and the support. The authors thank the ZEA-3 for the measurement of the NMR spectra. V.B.L. and L.M. acknowledges the support of the Elite Network Bavaria.

Conflict of interest

The authors declare no conflict of interest.

Keywords: assembly · block copolymers · nanoparticles · nanostructures

How to cite: *Angew. Chem. Int. Ed.* **2019**, *58*, 8541–8545
Angew. Chem. **2019**, *131*, 8629–8633

[1] M. A. Boles, M. Engel, D. V. Talapin, *Chem. Rev.* **2016**, *116*, 11220–11289.

[2] a) M. W. Matsen, F. S. Bates, *Macromolecules* **1996**, *29*, 7641–7644; b) S. Förster, T. Plantenberg, *Angew. Chem. Int. Ed.* **2002**, *41*, 688–714; *Angew. Chem.* **2002**, *114*, 712–739; c) A. C. Balasz, T. Emrick, T. P. Russell, *Science* **2006**, *314*, 1107–1110; d) M. R. Bockstaller, R. A. Mickiewicz, E. L. Thomas, *Adv. Mater.* **2005**, *17*, 1331–1349; e) M. Yoo, S. Kim, J. Bang, *J. Polym. Sci. Part B* **2013**, *51*, 494–507; f) J. Kao, K. Thorkelsson, P. Bai, B. J. Rancatore, T. Xu, *Chem. Soc. Rev.* **2013**, *42*, 2654–2678.

[3] a) J. J. Chiu, B. J. Kim, E. J. Kramer, D. J. Pine, *J. Am. Chem. Soc.* **2005**, *127*, 5036–5037; b) B. J. Kim, J. J. Chiu, G.-R. Yi, D. J. Pine, E. J. Kramer, *Adv. Mater.* **2005**, *17*, 2618–2622; c) B. J. Kim, J. Bang, C. J. Hawker, E. J. Kramer, *Macromolecules* **2006**, *39*, 4108–4114; d) B. J. Kim, S. Given-Beck, J. Bang, C. J. Hawker, E. J. Kramer, *Macromolecules* **2007**, *40*, 1796–1798; e) B. J. Kim, J. Bang, C. J. Hawker, J. J. Chiu, D. J. Pine, S. G. Jang, S.-M. Yang, E. J. Kramer, *Langmuir* **2007**, *23*, 12693–12703.

[4] a) B. Hamdoun, D. Ausserré, S. Joly, Y. Gallot, V. Cabuil, C. Clinard, *J. Phys. II* **1996**, *6*, 493–501; b) B. Hamdoun, D. Ausserré, S. Joly, *J. Phys. II* **1996**, *6*, 503–510; c) S. Förster, M. Antonietti, *Adv. Mater.* **1998**, *10*, 195–217.

[5] a) R. B. Thompson, V. V. Ginzburg, M. W. Matsen, A. C. Balasz, *Science* **2001**, *292*, 2469–2472; b) J. U. Kim, B. O'Shaughnessy, *Phys. Rev. Lett.* **2002**, *89*, 238301; c) J. Huh, V. V. Ginzburg, A. C. Balasz, *Macromolecules* **2000**, *33*, 8085–8096; d) J. Y. Lee, R. B. Thompson, D. Jasnow, A. C. Balasz, *Phys. Rev. Lett.* **2002**, *89*, 155503; e) R. Sknepnek, J. A. Anderson, M. H. Lamm, J. Schmalian, A. Travesset, *ACS Nano* **2008**, *2*, 1259–1265; f) M. K. Gaines, S. D. Smith, J. Samseth, M. R. Bockstaller, R. B. Thompson, K. O. Rasmussen, R. J. Spontak, *Soft Matter* **2008**, *4*, 1609–1612.

[6] a) Y. Lin, A. Böker, J. He, K. Still, H. Xiang, C. Abetz, X. Li, J. Wang, T. Emrick, S. Long, Q. Wang, A. Balazs, T. P. Russell, *Nature* **2005**, *434*, 55–59; b) M. R. Bockstaller, Y. Lapetnikov, S. Margel, E. L. Thomas, *J. Am. Chem. Soc.* **2003**, *125*, 5276–5277; c) D.-P. Song, C. Li, N. S. Colella, W. Xie, S. Li, X. Lu, S. Gido, J.-H. Lee, J. J. Watkins, *J. Am. Chem. Soc.* **2015**, *137*, 12510–12513; d) Z. Li, K. Hur, H. Sai, T. Higuchi, A. Takahara, H. Jinnai, S. M. Gruner, U. Wiesner, *Nat. Commun.* **2014**, *5*, 3247; e) M. S. Onses, L. Wan, X. Liu, N. B. Kiremitler, H. Yilmaz, P. F. Nealey, *ACS Macro Lett.* **2015**, *4*, 1356–1361; f) J. G. Son, W. K. Bae, H. Kang, P. F. Nealey, K. Char, *ACS Nano* **2009**, *3*, 3927–3934; g) S.-S. Kim, B.-H. Sohn, *RSC Adv.* **2016**, *6*, 41331–41339.

[7] J. Liu, Y. Gao, D. Cao, L. Zhang, Z. Guo, *Langmuir* **2011**, *27*, 7926–7933.

[8] a) Y. Zhao, K. Thorkelsson, A. J. Mastroianni, T. Schilling, J. M. Luther, B. J. Rancatore, K. Matsunaga, H. Jinnai, Y. Wu, D. Poulsen, J. M. J. Frechet, A. P. Alivisatos, T. Xu, *Nat. Mater.* **2009**, *8*, 979–985; b) Y. Gai, Y. Lin, D.-P. Song, B. M. Yavitt, J. J. Watkins, *Macromolecules* **2016**, *49*, 3352–3360; c) L. Yao, Y. Lin, J. J. Watkins, *Macromolecules* **2014**, *47*, 1844–1849; d) J. Kao, P. Bai, V. P. Chuang, Z. Jiang, P. Ercius, T. Xu, *Nano Lett.* **2012**, *12*, 2610–2618.

[9] S. C. Warren, L. C. Messina, L. S. Slaughter, M. Kamperman, Q. Zhou, S. M. Gruner, F. J. DiSalvo, U. Wiesner, *Science* **2008**, *320*, 1748–1752.

[10] a) P. Akcora, H. Liu, S. K. Kumar, J. Moll, Y. Li, B. C. Benicewicz, L. S. Schadler, D. Acehan, A. Z. Panagiotopoulos, V. Pryamitsyn, V. Ganesan, J. Ilavsky, P. Thiyagarajan, R. H. Colby, J. F. Douglas, *Nat. Mater.* **2009**, *8*, 354–359; b) S. Fischer, A. Salcher, A. Kornowski, H. Weller, S. Förster, *Angew. Chem. Int. Ed.* **2011**, *50*, 7811–7814; *Angew. Chem.* **2011**, *123*, 7957–7960.

[11] a) M. Yoo, S. Kim, J. Lim, E. J. Kramer, C. J. Hawker, B. J. Kim, J. Bang, *Macromolecules* **2010**, *43*, 3570–3575; b) J. Lim, H. Yang, K. Paek, C.-H. Cho, S. Kim, J. Bang, B. J. Kim, *J. Polym. Sci. Part A* **2011**, *49*, 3464–3474; c) S. G. Jang, A. Khan, M. D. Dimitriou, B. J. Kim, N. A. Lynd, E. J. Kramer, C. J. Hawker, *Soft Matter* **2011**, *7*, 6255–6263; d) E. Pöselt, C. Schmidtke, S. Fischer, K. Peldschus, J. Salamon, H. Kloust, H. Tran, A. Pietsch, M. Heine, G. Adam, U. Schumacher, C. Wagener, S. Förster, H. Weller, *ACS Nano* **2012**, *6*, 3346–3355; e) C. Schmidtke, E. Pöselt, J. Ostermann, A. Pietsch, H. Kloust, H. Tran, T. Schotten, N. G. Bastus, R. Eggers, H. Weller, *Nanoscale* **2013**, *5*, 7433–7444; f) A. Feld, R. Koll, L. S. Fruhner, M. Krutyeva, W. Pyckhout-Hintzen, C. Weiß, H. Heller, A. Weimer, C. Schmidtke, M.-S. Appavou, E. Kentzinger, J. Allgaier, H. Weller, *ACS Nano* **2017**, *11*, 3767–3775.

[12] a) M. C. Orilall, U. Wiesner, *Chem. Soc. Rev.* **2011**, *40*, 520–535; b) R. Shenhar, T. B. Norsten, V. M. Rotello, *Adv. Mater.* **2005**, *17*, 657–669.

[13] R. Glass, M. Möller, J. P. Spatz, *Nanotechnology* **2003**, *14*, 1153–1160; M. Faustini, A. Capobianchi, G. Varvaro, D. Grosso, *Chem. Mater.* **2012**, *24*, 1072–1079; B. Basly, T. Alnasser, K. Aissou, G. Fleury, G. Pecastaings, G. Hadziioannou, E. Duguet, G. Goglio, S. Mornet, *Langmuir* **2015**, *31*, 6675–6680; K. Aissou, T. Alnasser, G. Pecastaings, G. Goglio, O. Toulemonde, S. Mornet, G. Fleury, G. Hadziioannou, *J. Mater. Chem. C* **2013**, *1*, 1317–1321.

[14] A. K. Khandpur, S. Förster, F. S. Bates, I. W. Hamley, A. J. Ryan, W. Bras, K. Almdal, K. Mortensen, *Macromolecules* **1995**, *28*, 8796–8806.

[15] S. Ehlert, S. Mehdizadeh Taheri, D. Pirner, M. Drechlser, H.-W. Schmidt, S. Förster, *ACS Nano* **2014**, *8*, 6114–6122.

[16] M. A. Hines, G. D. Scholes, *Adv. Mater.* **2003**, *15*, 1844–1849.

[17] S. Ehlert, T. Lunkenbein, J. Breu, S. Förster, *Colloids Surf. A* **2014**, *444*, 76–80.

[18] J. Park, K. An, Y. Hwang, J.-G. Park, H.-J. Noh, J.-Y. Kim, J.-H. Park, N.-M. Hwang, T. Hyeon, *Nat. Mater.* **2004**, *3*, 891–895.

[19] A. Shavel, M. Ibánez, Z. Luo, J. De Roo, A. Carrete, M. Dimitrievska, A. Genc, M. Meyns, A. Pérez-Rodriguez, M. V. Kovalenko, J. Arbiol, A. Cabot, *Chem. Mater.* **2016**, *28*, 720–726.

[20] M. S. Nikolic, C. Olsson, A. Salcher, A. Kornowski, A. Rank, R. Schubert, A. Frömsdorf, H. Weller, S. Förster, *Angew. Chem. Int. Ed.* **2009**, *48*, 2752–2754; *Angew. Chem.* **2009**, *121*, 2790–2792.

[21] M. Daoud, J. P. Cotton, *J. Phys. France* **1982**, *43*, 531–538.

Manuscript received: February 13, 2019
Accepted manuscript online: April 10, 2019
Version of record online: May 13, 2019

 © 2019 Wiley-VCH Verlag GmbH & Co. KGaA, Weinheim